Revised theory of resonant degenerate four-wave mixing with broad-bandwidth lasers

J. Cooper
Joint Institute for Laboratory Astrophysics, University of Colorado and National Institute of Standards and Technology, Boulder, Colorado 80309-0440

A. Charlton,* D. R. Meacher, and P. Ewart
Clarendon Laboratory, University of Oxford, Parks Road, Oxford, OX1 3PU, United Kingdom

G. Alber
Faculty of Physics, Albert Ludwigs University, Hermann Herder Strasse 3D, 7800 Freiburg, Federal Republic of Germany
(Received 16 May 1989)

We present a revision of the theory of finite laser bandwidth effects on degenerate four-wave mixing (DFWM) of Alber, Cooper, and Ewart (ACE) [Phys. Rev. A **31**, 2344 (1985)]. The same model is used for intense, broad-bandwidth pump lasers interacting with a weak monochromatic probe in a medium composed of two-level atoms. The density-matrix equations describing the time evolution of the atomic polarization coupled to fluctuating fields are solved using an appropriate decorrelation approximation. A steady-state analytical solution is found for resonant and near-resonant DFWM, for intensities that do not saturate the medium. For more intense fields it is found to be necessary to form a more complicated set of differential equations for all products of the field and atomic density-matrix elements. The results show that as in the ACE theory, increasing the bandwidth b leads to an increased effective saturation intensity. However, we find the DFWM reflectivity scales as $1/b^2$ when the probe is monochromatic and not $1/b$ as in the ACE theory. Furthermore, the saturation behavior of nonresonant DFWM is found to differ from the predictions of ACE. Atomic motion effects are shown to yield a Doppler-broadened line shape and also to affect the saturation behavior of the signal.

I. INTRODUCTION

In a recent paper by Alber, Cooper, and Ewart[1] (referred to hereafter as ACE) a theory of resonant degenerate four-wave mixing with broad-bandwidth lasers was presented. The procedure adopted there was to calculate the density-matrix elements describing the nonlinear polarization generated by the interaction of broadband fluctuating laser fields with a two-level atom. The set of coupled differential equations describing the evolution of the density matrix were solved by a Laplace transform method where resonant terms to all orders in the intense pump fields, but only first order in the weak probe field, were included.

This method found the steady-state solution of the Laplace transformed equations and then formed the desired product of the required density-matrix elements averaged over the field fluctuations using a kind of decorrelation approximation. The adopted solution, however, did not properly deal with the fact that this product of density-matrix elements is determined by a convolution of the corresponding Laplace transformed quantities. In addition, the density-matrix equations of ACE [Eq. (2)] omitted two seemingly lower-order terms involving population differences, one of which cannot properly be neglected in the strong fields that produce saturation of the medium. In this paper we present firstly a solution valid for low-intensity pump fields, which is obtained by solving the density-matrix equations in the time domain. The decorrelation approximation is applied to products of fields and population terms in a way by which the essential physics of the procedure is also made more apparent and consistent. Secondly, the more general case of arbitrary pump intensities is treated by solving product-density matrix equations in the time domain with the help of a procedure that can easily be applied to phase diffusion or chaotic fields. For broadband radiation both types of field fluctuation lead to the same result which is equivalent to a decorrelation approximation for the product-density matrix equations.

The general area of optical phase conjugation by degenerate four-wave mixing (DFWM) has been reviewed in a book edited by Fisher.[2] The effects of finite laser bandwidth on nonlinear optical processes have been studied theoretically and experimentally in only a few cases (see ACE for references). Such effects on optical parametric processes have been reviewed by Reintjes.[3] More recently, the effects of field fluctuations, photon statistics, and mode beating have received attention in the areas of stimulated scattering processes such as coherent anti-Stokes Raman scattering (CARS).[4] A particular problem of calculating the signal in DFWM with broad-bandwidth lasers arises from the geometry of the three input waves. The two strong pump waves are counterpropagating and with their interaction with the probe beam give a spatial modulation of the field amplitudes. Furthermore, the stochastic fluctuations of the driving field amplitudes lead to a similar kind of fluctuation in the atomic polarization. It is the simultaneous averaging of both space and time variations of the atom-field products, determining the size of the generated fourth wave, that lies at the heart of the problem. The general case of arbitrary intensities and arbitrary bandwidths is, at present, an almost computationally intractable problem. In this paper we consider the same situation as that discussed by ACE, viz., intense broad-bandwidth pump waves interacting with a weak probe wave, which may also exhibit fluctuations, in a nonlinear medium composed of two-level atoms. In Sec. II we define the basic equations, initially for the coherent case (monochromatic pump waves) and then consider how their solution is modified in the incoherent case. The solution for very large bandwidths in the steady state is presented in Sec. III where we outline our procedure for averaging over the laser fluctuations with the help of a decorrelation approximation. In Sec. IV we discuss the results of the present work for the cases of exactly resonant DFWM and for situations where the detuning Δ is either less than or greater than the laser bandwidth b. The effect of atomic motion on the line shape and the saturation behavior of the signal are also discussed.

II. BASIC EQUATIONS

We consider the same four-wave mixing situation as that treated in the ACE theory, and so the assumptions and definitions will be outlined only briefly here for convenience. A medium of two-level atoms is traversed by two intense pump waves and a weak probe wave as shown in Fig. 1. Initially we consider *coherent* fields described by

$$E(\mathbf{x},t)=\sum_{j=1}^{3}\epsilon_j(\mathbf{x},t)e^{-i(\omega_j t-\mathbf{k}_j\cdot\mathbf{x})}+\text{c.c.} \tag{1}$$

The frequencies and wave vectors are given by $\omega_1=\omega_2,\omega_3$ and $-\mathbf{k}_1=\mathbf{k}_2,\mathbf{k}_3$, respectively. $\epsilon_j(\mathbf{x},t)$, $j=1$, 2, and 3, are the slowly varying field amplitudes. The pump waves, of equal amplitude, $\epsilon_1(\mathbf{x},t)=\epsilon_2(\mathbf{x},t)$, are tuned close to the frequency of the transition between the ground $|g\rangle$ and excited state $|e\rangle$, which have energies E_g and E_e, respectively. The detuning of the pump waves is

$$\Delta=(E_g+\hbar\omega_1-E_e)/\hbar \ .$$

The detuning of the probe wave Δ_2 and the generated fourth wave Δ_3 are given by

$$\Delta_2=-(-E_g-\hbar\omega_3+E_e)/\hbar \ ,$$

$$\Delta_3=(E_g+2\hbar\omega_1-\hbar\omega_3-E_e)/\hbar \ .$$

The pump-probe detuning δ is simply

$$\delta=(\omega_1-\omega_3) \ .$$

The interaction of the field with the atom is characterized by the Rabi frequency $\Omega(\mathbf{x})$, determined by the atomic dipole moment $\langle e|\boldsymbol{\mu}|g\rangle\equiv\mu_{eg}$. Taking the field amplitudes ϵ_j to be time and space independent, the probe field gives $\Omega_3=(2/\hbar)\langle e|\boldsymbol{\mu}|g\rangle\epsilon_3$, which is independent of position. However, the counterpropagating pump fields have a standing-wave spatial modulation, so

$$\Omega(\mathbf{x})=(2/\hbar)\langle e|\boldsymbol{\mu}|g\rangle 2\epsilon_1\cos(\mathbf{k}_1\cdot\mathbf{x}) \ . \tag{2}$$

The response of the atomic system is described by the macroscopic density operator $\rho(\mathbf{x},t)$. Within the rotating-wave approximation the slowly varying density-matrix elements

$$\rho_{ij}^{n,m}(\mathbf{x},t),\quad i,j=g,e$$

are given by

$$\rho(\mathbf{x},t)=\sum_{n,m=-\infty}^{\infty}\rho_{ij}^{n,m}(\mathbf{x},t)e^{-in\omega_1 t}e^{-im(\omega_3 t-\mathbf{k}_3\cdot\mathbf{x})} \ . \tag{3}$$

The longitudinal and transverse relaxation rates are given by κ and Γ, respectively, where $\Gamma=(\gamma+\kappa/2)$ and γ is the collisional dephasing rate. The evolution of the slowly varying density-matrix elements is described by the following system of equations:

$$\left[\frac{d}{dt}+\kappa\right](\rho_{gg}^{0,0}-\rho_{ee}^{0,0})(\mathbf{x},t)=\kappa-2\,\mathrm{Im}[\Omega^*(\mathbf{x})\rho_{eg}^{1,0}(\mathbf{x},t)] \ , \tag{4a}$$

$$\begin{aligned}\left[\frac{d}{dt}-i\Delta+\Gamma\right]\rho_{eg}^{1,0}(\mathbf{x},t)&=(i/2)\Omega(\mathbf{x})(\rho_{gg}^{0,0}-\rho_{ee}^{0,0})(\mathbf{x},t)\\&\quad+(i/2)\Omega_3(\rho_{gg}^{1,-1}-\rho_{ee}^{1,-1})(\mathbf{x},t) \ ,\end{aligned} \tag{4b}$$

$$\begin{aligned}\left[\frac{d}{dt}+i\Delta_2+\Gamma\right]\rho_{ge}^{0,-1}(\mathbf{x},t)&\\=(-i/2)\Omega_3^*(\rho_{gg}^{0,0}-\rho_{ee}^{0,0})(\mathbf{x},t)&\\-(i/2)\Omega^*(\mathbf{x})(\rho_{gg}^{1,-1}-\rho_{ee}^{1,-1})(\mathbf{x},t) \ ,&\end{aligned} \tag{4c}$$

$$\begin{aligned}\left[\frac{d}{dt}-i\delta+\kappa\right](\rho_{gg}^{1,-1}-\rho_{ee}^{1,-1})(\mathbf{x},t)&\\=i\Omega^*(\mathbf{x})\rho_{eg}^{2,-1}(\mathbf{x},t)&\\-i\Omega(\mathbf{x})\rho_{ge}^{0,-1}(\mathbf{x},t)+i\Omega_3^*\rho_{eg}^{1,0}(\mathbf{x},t) \ ,&\end{aligned} \tag{4d}$$

$$\begin{aligned}\left[\frac{d}{dt}-i\Delta_3+\Gamma\right]\rho_{eg}^{2,-1}(\mathbf{x},t)&\\=(i/2)\Omega(\mathbf{x})(\rho_{gg}^{1,-1}-\rho_{ee}^{1,-1})(\mathbf{x},t) \ .&\end{aligned} \tag{4e}$$

In these equations we have ignored all loss mechanisms from the two-level system. The second term on the right-hand side of Eq. (4b) involving Ω_3 leads to a term in the final solution, which is small compared to the other terms that involve $\Omega(\mathbf{x})$ and so may be neglected. However, the second term on the right-hand side of Eq. (4c) is coupled to the strong-field term $\Omega^*(\mathbf{x})$ and is retained here since it becomes important when the medium is saturated at high intensities. Solving these equations with the condition that all atoms are initially in the ground state enables the product

$$\rho_{eg}^{2,-1}(\mathbf{x},t)[\rho_{eg}^{2,-1}(\mathbf{x}',t)]^* \ ,$$

which determines the size of the generated signal intensity to be found. The intensity of the generated signal I_4 is then given by

$$I_4=\frac{1}{2\epsilon_0 c}(|\mathbf{k}_4|cN)^2|\mu_{eg}|^2 \times\langle \rho_{eg}^{2,-1}(\mathbf{x},t\rightarrow\infty)[\rho_{eg}^{2,-1}(\mathbf{x}',t\rightarrow\infty)]^*\rangle_s \ . \quad (5)$$

$\langle\ \rangle_s$ indicates a spatial average over $\mathbf{x}$ and $\mathbf{x}'$.[5] N is the number of atoms in the interaction region divided by the cross section of the weak probe beam. Within the approximation that we ignore all propagation effects such as absorption of pump, probe, and generated waves, we obtain for the monochromatic case a DFWM reflectivity R, equivalent to the usual results[5] given by

$$R\propto|(B_c\overline{\Omega}^2L)|^2\left|\frac{1}{(\beta_c-\alpha_c)}\left[\left[\frac{\beta_c}{\beta_c+\Omega^2}\right]^{1/2}-\left[\frac{\alpha_c}{\alpha_c+\Omega^2}\right]^{1/2}\right]\right|^2, \quad (6)$$

where

$$B_c=\frac{(-i/4)(\Gamma+i\Delta)(2\Gamma-i\delta)\kappa}{(\Gamma-i\delta)\Gamma},$$

$$\alpha_c=\frac{[\Gamma+i(\Delta-\delta)][\Gamma-i(\Delta+\delta)][\kappa-i\delta]}{\Gamma-i\delta},$$

$$\beta_c=\frac{(\Delta^2+\Gamma^2)\kappa}{\Gamma},$$

and

$$\overline{\Omega}=(2/\hbar)\langle e|\boldsymbol{\mu}|g\rangle 2\epsilon_1 \ .$$

For the *incoherent* case the generated signal is again found from the product

$$\langle\rho_{eg}^{2,-1}(\mathbf{x},t)[\rho_{eg}^{2,-1}(\mathbf{x}',t)]^*\rangle_f \ ,$$

where $\langle\ \rangle_f$ denotes, in addition, the average over the field fluctuations. In the incoherent case the amplitudes of the exciting laser fields $\epsilon_j(t)$, $j=1,2,3$ [see Eq. (1)] are subject to stochastic phase and/or amplitude fluctuations. The mean generated intensity $\langle I_4\rangle$ is then obtained from Eq. (5) by averaging over these laser fluctuations. It is the simultaneous averaging over space and the laser fluctuations that complicates this problem.

In general, it is difficult to calculate $\langle I_4\rangle$. However, under certain conditions it is possible to obtain analytical solutions. As in the study by ACE, in the following, we particularly concentrate on situations where the bandwidths of the exciting laser fields are much larger than all other rates determining the time evolution of the nonlinear medium. Furthermore, we assume that the right and left propagating fields are statistically independent, have the same mean intensity, and are characterized by Lorentzian spectra of bandwidth b. We also restrict ourselves to situations where the characteristic interaction lengths are small in the sense $L<(c/nb)$ (n is the index of refraction) so that the retardation effects may be neglected. Due to the fact that we are interested in the large-bandwidth case, it does not matter which model we use for describing the laser fluctuations [e.g., phase-diffusion model (PDM) or chaotic field (CF)] as long as their spectra are identical (see Appendix B).

III. LARGE-BANDWIDTH SOLUTION

For the incoherent case the simultaneous averaging over the temporal fluctuations of the field and the spatial variation of the polarization must be carried out with due regard to the correlations of atom-field variables inherent in the required product of density-matrix elements. In this section we present first a solution for the case of low-intensity broadband pumps characterized by a chaotic or phase-diffusing field and a monochromatic probe field. This example illustrates the procedure of making a decorrelation approximation simultaneously for all the coupled density-matrix elements. In this case it is possible to reach an analytical solution. For arbitrarily intense pump fields this procedure is more complicated. In this second case we present also a more generally valid solution using the Fokker-Planck operator which, for the broadband cases discussed here, is applicable to both chaotic and phase-diffusing fields.

We begin by replacing the field description of Eq. (1) by that of a fluctuating field, characteristic of broad-bandwidth pulsed lasers. The Rabi frequency of Eq. (2) is also changed, since, for the counterpropagating uncorrelated fields to be considered here, there will be no steady-state standing-wave pattern established by the pump beams. With these changes, Eqs. (4) may be solved in the time domain, and the averaged product,

$$\langle\rho_{eg}^{2,-1}(\mathbf{x},t)[\rho_{eg}^{2,-1}(\mathbf{x},t)]^*\rangle_f \ ,$$

expressed in terms of products of atomic parameters which have been appropriately decorrelated from the field variables.

We consider the incoherent laser fields to be described, in the same manner as ACE, by

$$\hat{\mathbf{e}}E(\mathbf{x},t)=\sum_{\mu}^{\infty}(\epsilon_\mu^r e^{i\mathbf{k}_1\cdot\mathbf{x}}+\epsilon_\mu^l e^{-i\mathbf{k}_1\cdot\mathbf{x}})\hat{\mathbf{e}}e^{-i(\overline{\omega}_\mu-\omega_1)t}\times e^{-i\omega_1 t}+\text{c.c.} \quad (7)$$

The expression represents right (r) and left (l) propagating fields, polarized along $\hat{\mathbf{e}}$, each consisting of an infinite number of modes μ, with amplitudes $\epsilon_\mu^{r,l}$, and frequency $\overline{\omega}_\mu$. As in ACE we take the fields to be uncorrelated:

$$\langle\epsilon_\mu^i(\epsilon_\nu^j)^*\rangle=0 \ \text{ if } i\neq j,\ \mu\neq\nu,\ i,j=r,l \ .$$

The time-independent field amplitude of Eq. (7) defines the new Rabi frequency $\Omega(\mathbf{x},t)$ given by

$$\Omega(\mathbf{x},t)=(2/\hbar)\langle e|\boldsymbol{\mu}\cdot\hat{\mathbf{e}}|g\rangle\sum_{\mu}^{\infty}(\epsilon_\mu^r e^{i\mathbf{k}_1\cdot\mathbf{x}}+\epsilon_\mu^l e^{-i\mathbf{k}_1\cdot\mathbf{x}})\times e^{-i(\overline{\omega}_\mu-\omega_1)t} \ . \quad (8)$$

We treat the case where right and left propagating modes of the pump waves have the same mean frequency ω_1 and the same mean intensity

$$\sum_{\mu} |\epsilon_\mu^r|^2 = \sum_{\mu} |\epsilon_\mu^l|^2 .$$

We further consider the pump fields to have a Lorentzian spectrum of width b [half-width at half maximum (HWHM)] and the probe field to be weak and monochromatic. Most importantly, we consider the bandwidth b to exceed all other relaxation rates of the system:

$$b \gg [\langle |\Omega(\mathbf{x},t)|^2 \rangle]^{1/2}, \kappa, \gamma .$$

We simplify the notation by writing

$$\rho^{0,0}(t) = (\rho_{gg}^{0,0} - \rho_{ee}^{0,0})(\mathbf{x},t)$$

and

$$\rho^{1,-1}(t) = (\rho_{gg}^{1,-1} - \rho_{ee}^{1,-1})(\mathbf{x},t) ,$$

also

$$\beta = \Gamma - i\Delta ,$$

$$\beta_2 = \Gamma - i\Delta_2 ,$$

$$\beta_3 = \Gamma - i\Delta_3 ,$$

$$\alpha = \kappa - i\delta .$$

Now formally integrating Eqs. (4), neglecting the term in Ω_3 in (4b), gives

$$\rho^{0,0}(t) = 1 - \left[\mathrm{Re} \int_{-\infty}^{t} dt_1 \int_{-\infty}^{t_1} dt_2 e^{-\beta(t_1-t_2)} e^{\kappa(t_1-t)} \Omega^*(t_1)\Omega(t_2)\rho^{0,0}(t_2) \right] , \tag{9}$$

$$\rho^{1,-1}(t) + \frac{1}{2} \left[\int_{-\infty}^{t} dt_1 \int_{-\infty}^{t_1} dt_2 e^{-\alpha(t-t_1)} [e^{\beta_3(t_2-t_2)} \Omega^*(t_1)\Omega(t_2) + e^{\beta_2^*(t_2-t_1)} \Omega(t_1)\Omega^*(t_2)] \rho^{1,-1}(t_2) \right]$$
$$= (-i/2) \left[\int_{-\infty}^{t} dt_1 \int_{-\infty}^{t_1} dt_2 e^{-\alpha(t-t_1)} [e^{-\beta(t_1-t_2)} \Omega_3^* \Omega(t_2) + e^{\beta_2^*(t_2-t_1)} \Omega_3^* \Omega(t_1)] \rho^{0,0}(t_2) \right] , \tag{10}$$

and

$$\rho_{eg}^{2,-1}(t) = (i/2) e^{-\beta_3 t} \int_{-\infty}^{t} dt_1 e^{\beta_3 t_1} \Omega(t_1) \rho^{1,-1}(t_1) . \tag{11}$$

From these equations we see that the desired product

$$\langle \rho_{eg}^{2,-1}(\mathbf{x},t)[\rho_{eg}^{2,-1}(\mathbf{x},t)]^* \rangle_f$$

will involve time-averaged products of population terms and field terms which are, in general, correlated. However, we note that the average population terms $\rho^{0,0}$ and $\rho^{1,-1}$ will vary on a time scale of $1/\kappa$ whereas the correlation time of the fields is $1/b$ which is much shorter. Under these conditions, we may decorrelate all products of field and population terms.

We consider first the special case of low-intensity pump beams $|\Omega| \ll \kappa$ for which we can simplify Eqs. (9)–(11) as

$$\rho^{0,0}(\mathbf{x},t_4) = 1 , \tag{12}$$

$$\rho^{1,-1}(\mathbf{x},t_1) = -\frac{i}{2} \Omega_3^* \int_{-\infty}^{t_1} dt_3 \int_{-\infty}^{t_3} dt_4 [\Omega(\mathbf{x},t_3) e^{-\beta_2^*(t_3-t_4)} + \Omega(\mathbf{x},t_4) e^{-\beta(t_3-t_4)}] e^{-\alpha(t_1-t_3)} \rho^{0,0}(\mathbf{x},t_4) , \tag{13}$$

$$\rho_{eg}^{2,-1}(\mathbf{x},t) = \frac{i}{2} e^{-\beta_3 t} \int_{-\infty}^{t} dt_1 \Omega(\mathbf{x},t_1) \rho^{1,-1}(\mathbf{x},t_1) e^{\beta_3 t_1} . \tag{14}$$

Equations (12)–(14) can be readily incorporated into a single expression for $\rho^{2,-1}(\mathbf{x},t)$ and the desired product formed. This product is simply a six-dimensional time integral which can be decorrelated and averaged by writing the field terms as

$$\Omega(\mathbf{x},t) = \Omega^r(t) e^{i\mathbf{k}\cdot\mathbf{x}} + \Omega^l(t) e^{-i\mathbf{k}\cdot\mathbf{x}} .$$

Remembering that right and left propagating modes are uncorrelated, we find in the limit that $b \gg \Delta, \Delta_2, \delta$, the solution for the desired product is [see Eq. (A4), Appendix A],

$$\langle \rho_{eg}^{2,-1}(\mathbf{x},t)[\rho_{eg}^{2,-1}(\mathbf{x}',t)]^* \rangle_f = \frac{|\Omega_3|^2 \Omega^4}{8\Gamma\kappa b^2} \left[\frac{1}{\Gamma^2 + \Delta_2^2} + \frac{1}{\Gamma} \frac{(\Gamma+\kappa)}{(\Gamma+\kappa)^2 + \Delta_2^2} \right] . \tag{15}$$

The generated signal I_4, and hence the DFWM reflectivity R, is found by integrating Eq. (15) over the interaction volume.

This method can not be used to treat the case of arbitrary field strengths since a sequential solution of Eqs. (9)–(11) requires sequential decorrelations to be made. In particular, it is not possible to decorrelate products like $\langle \rho^{0,0}(\mathbf{x},t)\Omega(\mathbf{x}',t_3)\Omega^*(\mathbf{x}',t_4) \rangle$ when $t > t_3$ and t_4 [since quantities depending on $\Omega^*(\mathbf{x},t_3)\Omega(\mathbf{x},t_4)$ are included in the expression for $\rho^{0,0}(\mathbf{x},t)$]. This essentially neglects important correlated terms inherent in the averaged product

$$\langle \rho_{eg}^{2,-1}(\mathbf{x},t)[\rho_{eg}^{2,-1}(\mathbf{x}',t)]^* \rangle_f ,$$

which cannot be ignored at high intensities. Instead, we adopt a different procedure that also allows us to treat a probe beam which has a finite bandwidth p. The mathematical manipulations are described more fully in Appendix B and the method is outlined as follows.

To simplify the notation even further we first reduce the notation for the density-matrix elements as follows:

$$\rho^{0,0}(\mathbf{x},t)\rightarrow\rho_0(\mathbf{x},t)\ ,$$

$$\rho_{eg}^{1,0}(\mathbf{x},t)\rightarrow\rho_1(\mathbf{x},t)\ ,$$

$$[\rho_{eg}^{1,0}(\mathbf{x},t)]^*\rightarrow\rho_2(\mathbf{x},t)\ ,$$

$$\rho_{eg}^{0,-1}(\mathbf{x},t)\rightarrow\rho_3(\mathbf{x},t)\ ,$$

$$\rho^{1,-1}(\mathbf{x},t)\rightarrow\rho_4(\mathbf{x},t)\ ,$$

$$\rho_{eg}^{2,-1}(\mathbf{x},t)\rightarrow\rho_5(\mathbf{x},t)\ .$$

Representing the products of these density-matrix elements by

$$A_{jk}\equiv\rho_j(\mathbf{x},t)[\rho_k(\mathbf{x}',t)]^*,\quad j,k=1,2,\ldots,5$$

we see the desired product will be denoted by $A_{55}(\mathbf{x},\mathbf{x}',t)$. These products are stochastic processes due to the fluctuating laser fields and a complete set of differential equations for them may be derived. The first few, which illustrate their structure, are

$$\left[\frac{d}{dt}+2\Gamma\right]A_{55}(\mathbf{x},\mathbf{x}',t)$$
$$=(i/2)[\Omega(\mathbf{x}',t)A_{45}(\mathbf{x},\mathbf{x}',t)-\Omega^*(\mathbf{x}',t)A_{54}(\mathbf{x},\mathbf{x}',t)]\ ,$$

$$\left[\frac{d}{dt}+(d^*+a)\right]A_{54}(\mathbf{x},\mathbf{x}',t)$$
$$=i[\Omega^*(\mathbf{x}',t)A_{55}(\mathbf{x},\mathbf{x}',t)+\Omega^*(x',t)A_{53}(\mathbf{x},\mathbf{x}',t)$$
$$-\Omega_3A_{51}(\mathbf{x},\mathbf{x}',t)+\tfrac{1}{2}\Omega(\mathbf{x},t)A_{44}(\mathbf{x},\mathbf{x}',t)]\ ,$$

$$\left[\frac{d}{dt}+(d+a^*)\right]A_{45}(\mathbf{x},\mathbf{x}',t)$$
$$=i[\Omega^*(\mathbf{x},t)A_{55}(\mathbf{x},\mathbf{x}',t)-\Omega(\mathbf{x},t)A_{35}(\mathbf{x},\mathbf{x}',t)$$
$$+\Omega_3^*A_{15}(\mathbf{x},\mathbf{x}',t)-\tfrac{1}{2}\Omega(\mathbf{x}',t)A_{44}(\mathbf{x},\mathbf{x}',t)]\ ,$$

and so on, where $a=\Gamma-i\Delta_3$ and $d=\kappa-i\delta$.

The equations for A_{54} and A_{45} may be formally integrated and substituted into the equation for $A_{55}(\mathbf{x},\mathbf{x}',t)$. The average over the field fluctuations is obtained with the aid of a decorrelation approximation, where, for example,

$$\langle\Omega^*(\mathbf{x}',t)\Omega(\mathbf{x},t')A_{44}(\mathbf{x},\mathbf{x}',t)\rangle$$
$$=\langle\Omega^*(\mathbf{x}',t)\Omega(\mathbf{x},t')\rangle\langle A_{44}(\mathbf{x},\mathbf{x}',t)\rangle$$
$$=2\cos[k(\mathbf{x}-\mathbf{x}')]|\Omega|^2e^{-b(t-t')}\langle A_{44}(\mathbf{x},\mathbf{x}',t)\rangle\ , \quad (16)$$

and

$$\langle\Omega(\mathbf{x},t)A_{15}(\mathbf{x},\mathbf{x}',t')\rangle=e^{-b(t-t')}\langle\Omega(\mathbf{x},t')A_{15}(\mathbf{x},\mathbf{x}',t')\rangle\ .$$

In this manner a set of equations for the product density matrices is obtained. Obtaining the solution for $\langle A_{55}(\mathbf{x},\mathbf{x}',t)\rangle$ is tedious, but may also be done numerically. The key point to note here is that the decorrelation is carried out simultaneously for all the coupled atom-field variables. In contrast with the $\langle\rho^{0,0}(t)\Omega(t_3)\Omega^*(t_4)\rangle$ case discussed previously, we now have, e.g., $A_{44}(\mathbf{x},\mathbf{x}',t)$ at time t', which does not depend on the interval $t'\rightarrow t$ and thus $\Omega^*(\mathbf{x}',t)\Omega(\mathbf{x},t')$ may be averaged separately for short correlation times (i.e., broadband radiation). This procedure for evaluating the product density-matrix elements is similar to the averaging methods outlined by Georges[6] and in the limit of large bandwidth is equivalent to his decorrelation approximation (which is valid for both phase diffusion and chaotic fields).

Alternatively, $\langle A_{55}(\mathbf{x},\mathbf{x}',t)\rangle$ may be calculated with the help of an eigenfunction expansion in terms of the eigenfunctions of the Fokker-Planck operator,[7] which describes the fluctuations of the pump (and probe) waves. If the fluctuation of the pump waves can be described, for example, by the phase-diffusion model, the Fokker-Planck operator is given by

$$L(\eta_1,\eta_2)=b\left[\frac{\partial^2}{\partial\eta_1^2}+\frac{\partial^2}{\partial\eta_2^2}\right]\ ,$$

with

$$\epsilon_j(t)=\epsilon_0e^{i\eta_j(t)},\quad j=1,2\ .$$

Its eigenvalues and eigenfunctions are determined by

$$L(\eta_1,\eta_2)\Pi_{n_1,n_2}(\eta_1,\eta_2)=\Lambda_{n_1,n_2}\Pi_{n_1,n_2}(\eta_1,\eta_2)\ , \quad (17a)$$

from which we find

$$\Pi_{n_1,n_2}(\eta_1,\eta_2)=\left[\frac{1}{\sqrt{2\pi}}\right]^2e^{-in_1\eta_1}e^{-in_2\eta_2} \quad (17b)$$

and

$$\Lambda_{n_1,n_2}=b(n_1^2+n_2^2),\quad n_1,n_2=0,\pm1,\ldots\ . \quad (17c)$$

Projecting the equations for $A_{ij}(\mathbf{x},\mathbf{x}',t)$ onto the eigenfunctions of the Fokker-Planck operator, we obtain an infinite system of equations for atom-field averages, which in the case of the PDM are defined by

$$A_{ij}^{(n_1,n_2)}(\mathbf{x},\mathbf{x}'t)$$
$$=\int_0^{2\pi}d\eta_1\int_0^{2\pi}d\eta_2\Pi_{n_1,n_2}^*(\eta_1,\eta_2)A_{ij}(\mathbf{x},\mathbf{x}'t)\ . \quad (17d)$$

The mean generated intensity can then be obtained from the relation

$$\langle A_{55}(\mathbf{x},\mathbf{x}',t)\rangle=A_{55}^{(0,0)}(\mathbf{x},\mathbf{x}',t\rightarrow\infty)/2\pi\ . \quad (18)$$

In the large-bandwidth approximation (which is valid for $b\gtrsim\Omega,\Gamma$) we keep only the couplings of $A_{55}^{(0,0)}(\mathbf{x},\mathbf{x}',t)$ to atom-field averages with $|n_1|,|n_2|\le1$, which allows us to obtain analytical expressions for $A_{55}^{(0,0)}(\mathbf{x},\mathbf{x}',t\rightarrow\infty)$. These equations are identical to those obtained from the decorrelation procedure of Eq. (16) discussed above (which, as mentioned, are equally valid for either phase diffusion or chaotic fields). Approximate expressions are given in Sec. IV, but it was also simple to numerically evaluate the 56 coupled equations for $A_{55}^{(0,0)}(\mathbf{x},\mathbf{x}',t)$. In

Appendix B we demonstrate this procedure in detail. However, due to the complexity of the complete set of equations we restrict ourselves there to the evaluation of

$$\langle [\rho_{gg}^{0,0}(\mathbf{x},t)-\rho_{ee}^{0,0}(\mathbf{x},t)][\rho_{gg}^{0,0}(\mathbf{x}',t)-\rho_{ee}^{0,0}(\mathbf{x}',t)]\rangle \ .$$

The evaluation of $\langle A_{55}(\mathbf{x},\mathbf{x}',t)\rangle$ proceeds along the same lines and is straightforward, but tedious, as mentioned above.

This solution agrees exactly with the analytic solution for low-intensity pump beams and can be applied to arbitrarily large intensities and detunings. The key to its success is the simultaneous decorrelation of all field terms from the density-matrix elements.

IV. RESULTS AND DISCUSSION

We now present our revised results on the generated four-wave mixing signal with broadband lasers and compare them with the result for the coherent case where the reflectivity R is given by Eq. (6). The generated signal in the case where both pump and probe fields are coherent is then

$$I_4=\frac{1}{2\epsilon_0 c}(|\mathbf{k}_4|cN)^2|\mu_{eg}|^2|\Omega_3|^2R \ . \qquad (19)$$

In the degenerate case ($\delta=0$) this reduces to the result of Ref. 4 and differs from the one in ACE due to the presence of the second term on the right-hand side of Eq. (4c), which actually cannot be neglected when the atomic transition $|g\rangle\to|e\rangle$ starts to saturate.

In the more general case of broadband pump waves and a weak probe beam of bandwidth p we obtain with the help of the procedure outlined above:

$$\langle \rho_{eg}^{2,-1}(\mathbf{x},t\to\infty)[\rho_{eg}^{2,-1}(\mathbf{x}',t\to\infty)]^*\rangle$$
$$=\frac{\kappa\vartheta}{2\Gamma^2}|\Omega_3|^2\cos^2[\mathbf{k}_1(\mathbf{x}-\mathbf{x}')]$$
$$\times\frac{2\,\mathrm{Re}(T_1+T_2)}{(1+2\vartheta)\left[1+\dfrac{\kappa\vartheta}{\Gamma}\right]-2\dfrac{\kappa\vartheta^2}{\Gamma}\cos^2[\mathbf{k}_1\cdot(\mathbf{x}-\mathbf{x}')]}\ , \qquad (20)$$

with

$$\vartheta=\frac{|\Omega|^2}{\kappa}\frac{b}{\Delta^2+b^2}\ ,$$

$$T_1=\frac{\Gamma}{\kappa}\frac{(1+T_3+T_4)c_2+T_3c_1}{(1+T_3+T_4)^2-T_3^2\cos^2[\mathbf{k}_1\cdot(\mathbf{x}-\mathbf{x}')]}\ ,$$

$$T_2=\left[\frac{\vartheta}{1+\dfrac{\kappa\vartheta}{\Gamma}}\right]\frac{(1+T_3+T_4)c_1+T_3c_2\cos^2[\mathbf{k}_1\cdot(\mathbf{x}-\mathbf{x}')]}{(1+T_3+T_4)^2-T_3^2\cos^2[\mathbf{k}_1\cdot(\mathbf{x}-\mathbf{x}')]}\ ,$$

$$T_3=\frac{|\Omega|^2}{i\Delta_2+\Gamma+\kappa+p}\left[\frac{1}{-i\delta+b}+\frac{1}{i(\Delta_2+\Delta)+b}\right],$$

$$T_4=\frac{|\Omega|^2}{i\Delta_2+\Gamma+\kappa+p}\left[\frac{1}{-i\delta+b}\right],$$

$$c_1=\frac{1}{i\Delta_2+\Gamma+\kappa+p}\left[\frac{1}{2}\langle A_{00}(\mathbf{x},\mathbf{x}',t\to\infty)\rangle+\frac{\kappa}{2}\frac{1}{i\Delta_2+\Gamma+p+\dfrac{|\Omega|^2}{-i\delta+b+p}}\times\left[\frac{1}{1+2\vartheta}\right]\right],$$

$$c_2=\frac{1}{i\Delta_2+\Gamma+\kappa+p}\frac{\dfrac{\kappa\vartheta}{2\Gamma}}{\left[1+\dfrac{\kappa\vartheta}{\Gamma}\right]}\langle A_{00}(\mathbf{x},\mathbf{x}',t\to\infty)\rangle\ ,$$

$$|\Omega|^2=\left\langle\left|\frac{2}{\hbar}\mu_{eg}\epsilon_1\right|^2\right\rangle\ ,$$

and $\langle A_{00}(\mathbf{x},\mathbf{x}',t\to\infty)\rangle$ defined in Appendix B [Eq. (B3)]. This result is valid for arbitrary bandwidths p of the weak probe beam, but only for large bandwidths b of the intense pump waves so that $b\gtrsim|\Delta|,|\delta|$. For $|\Delta|$ and $|\delta|$ greater than b, the equations for $A_{55}^{(0,0)}(\mathbf{x},\mathbf{x}',t)$, discussed in Sec. II, have to be evaluated numerically.

These results are shown in Fig. 1 which shows the resonant ($\Delta=0$) DFWM reflectivity R for monochromatic waves, calculated using Eq. (6) plotted logarithmically as a function of the parameter $|\Omega|^2/\kappa^2$, which is proportional to the pump intensity I_1. This result is identical to that of Ref. 5 and shows that for intensities in excess of the saturation value I_{sat}, $R\propto I^{-1}$.

The effects of broad pump laser bandwidth ($b/\kappa=10^2,10^3$) are shown by two additional curves in Fig. 1. In these curves also $\Delta=0$ and the probe is monochromatic. The general features of the response with broad-bandwidth pump fields are similar to those predicted in ACE, notably that increased bandwidth leads to a reduced efficiency for $I_1<I_{\mathrm{sat}}$ and I_{sat} increases in proportion to the pump bandwidth for $b\gg\Delta$. Qualitatively, the predictions of present work differ from those of ACE in that the reflectivity R scales as b^{-2} for $I_1\ll I_{\mathrm{sat}}$ and also $R\propto I^{-3/2}$ rather than I^{-2} for $I_1\gg I_{\mathrm{sat}}$. These pre-

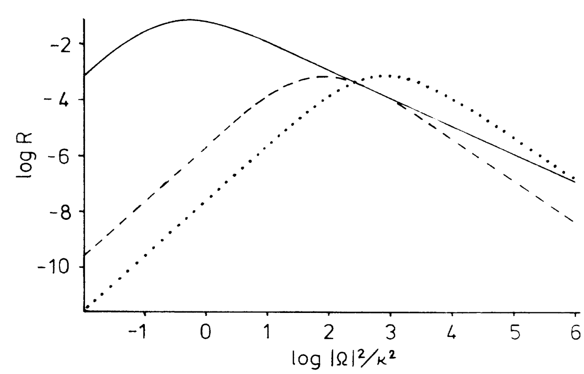

FIG. 1. Logarithmic plot of R against $|\Omega^2|/\kappa^2$ for $\Delta=0$ and probe bandwidth $p=0$. Pump bandwidths $b/\kappa=0$ (solid line), $b/\kappa=10^2$ (dashed line), and $b/\kappa=10^3$ (dotted line).

dictions are modified in the case where atomic motion effects are important and lead, as we shall show later, to a reflectivity decreasing with I^{-2} for $I_1 \gg I_{sat}$.

We consider now the case when the pump laser may be detuned from the atomic resonance, $\Delta \neq 0$. Two situations may be encountered where either the bandwidth exceeds the detuning, $\Delta < b$, when the approximate analytical solution is valid or the converse, $\Delta > b$, when the full numerical solution of the coupled equations must be used. In Fig. 2(a) we show the results for the former case for three values of $b > \Delta$. We observe the trend for the saturation intensity to increase with increasing bandwidth b. In Fig. 2(b) we show the predicted saturation behavior when b is increased from a value initially less than the detuning to a value greater than the detuning. We note that the saturation intensity is at first reduced for increasing bandwidth. This may be explained by a more effective overlap of the laser spectrum with the atomic resonance. As the bandwidth is increased further the improved overlap is less effective and the saturation intensity increases as before.

The discussion so far has considered the case of a coherent probe field $p=0$. However, the theory may easily be generalized to include the case of the finite probe bandwidth.

If p is large in the sense that $|\Omega|^2/pb \ll 1$ and $p \gg \Gamma, \kappa$, then $T_3, T_4 \ll 1$ and we obtain a relatively simple expression for the reflectivity (after integrating over $\mathbf{x}-\mathbf{x}'$)

$$R = \frac{\kappa\vartheta^2}{4\Gamma^2}\left[\frac{\Gamma+\kappa+p}{\Delta_2^2+(\Gamma+\kappa+p)^2}\right] \times \frac{1}{\left[(1+2\vartheta)^{3/2}\left[1+\frac{\kappa\vartheta}{\Gamma}\right]^{1/2}\right]} \times \frac{1}{\left[(1+2\vartheta)\left[1+\frac{\kappa\vartheta}{\Gamma}\right]-2\frac{\kappa}{\Gamma}\vartheta^2\right]^{3/2}} . \tag{21}$$

These approximations, Eqs. (20) and (21), have been checked numerically against the full solution of the coupled equations and have been shown to be in excellent agreement within their range of validity (i.e., $b > |\Delta|, |\delta|$). The approximate R, obtained after numerically integrating Eq. (20) over $(\mathbf{x}, \mathbf{x}')$, drops precipitously to zero outside of its range of validity, whereas the full numerical solution for R is well behaved for $\Omega \lesssim b$ irrespective of δ and Δ.

In most experimental situations $p=b$ and so we show in Figs. 3(a) and 3(b) the effects of detuning for this case. For clarity in these figures we calculate curves for values of $b/\kappa = 2.5\times10^2$, 10^3, and 10^4. Figure 3(a) shows the case where $b > \Delta$ (specifically $\Delta/\kappa = 10^2$). In Fig. 3(b) $\Delta/\kappa = 10^3$ and here we see the effect of b increasing from

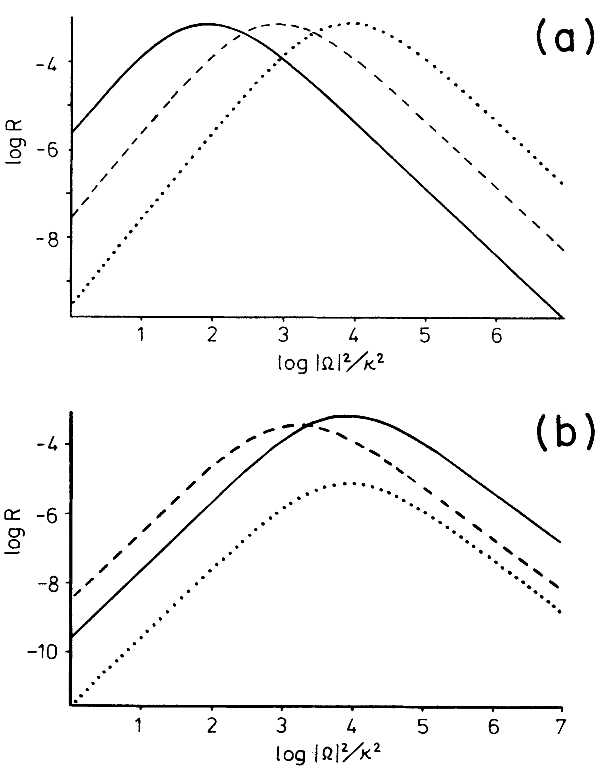

FIG. 2. Logarithmic plot of R against $|\Omega^2|/\kappa^2$ for probe bandwidth $p=0$ and pump bandwidth $b/\kappa=10^2$ (solid line), $b/\kappa=10^3$ (dashed line), and $b/\kappa=10^4$ (dotted line). (a) $\Delta/\kappa=0$ and (b) $\Delta/\kappa=10^3$.

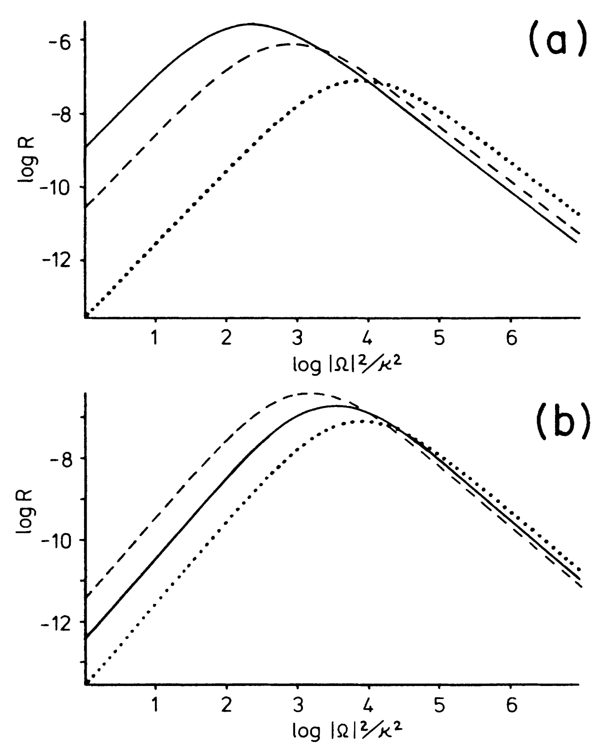

FIG. 3. Logarithmic plot of R against $|\Omega^2|/\kappa^2$ for equal probe and pump bandwidths $b/\kappa=2.5\times10^2$ (solid line), $b/\kappa=10^3$ (dashed line), and $b/\kappa=10^4$ (dotted line). (a) $\Delta/\kappa=10^2$ and (b) $\Delta/\kappa=10^3$.

$b < \Delta$ to $b > \Delta$.

In Fig. 4 we show the effect of a nonmonochromatic probe on the resonant ($\Delta=0$) reflectivity. By comparison with Fig. 2(a) where $p=0$, we see the result for a broad probe bandwidth $p=b$ for three values of b. In general, the response is modified in that the peak reflectivity now scales as p^{-1} and the reflectivity for $I_1 \ll I_{\rm sat}$ now varies as $b^{-2}p^{-1}$.

It is a complex problem to include effects of atomic motion in the case of intense pump waves. In the case of broad-bandwidth laser fields its effects are most significant if the weak probe beam has a small bandwidth p or is coherent. The effect of the motion is to replace $\mathbf{x}$ by $\mathbf{x}+\mathbf{v}t$, so that in the observable [Eq. (5)] $\rho_{eg}^{2,-1}(\mathbf{x},t\to\infty)$ has to be replaced by

$$\rho_{eg}^{2,-1}(\mathbf{x},t\to\infty)e^{i\mathbf{k}_4\cdot(\mathbf{x}+\mathbf{v}t)}$$

(with $\mathbf{k}_4=-\mathbf{k}_3$), and similarly for the complex-conjugate term $\mathbf{x}'$. An integration with respect to $\mathbf{v}$ and $\mathbf{v}'$ (or alternatively $\mathbf{v}$ and $\Delta\mathbf{v}=\mathbf{v}-\mathbf{v}'$) then has to be performed. In principle, the analysis, although very tedious, could be carried through in detail, however, qualitative results may easily be obtained. We assume that the Doppler width $\Delta\omega_D \simeq \mathbf{k}\cdot\mathbf{v}_{\rm av}$ (where $\mathbf{v}_{\rm av}$ is the mean thermal velocity) is large compared to κ but small compared to b.

Firstly, in order to ascertain the effect of the motion of the atoms we examine the denominators that occur in the low-field problem. Specifically, we find terms like $2\Gamma+i\mathbf{k}_3\cdot\Delta\mathbf{v}$, $2\kappa+i\mathbf{k}_3\cdot\Delta\mathbf{v}\pm\epsilon i\mathbf{k}_1\cdot\Delta\mathbf{v}$, $2\Gamma+i\epsilon\mathbf{k}_1\cdot\Delta\mathbf{v}$ (with $\epsilon=\pm1$), and so on. By examining the poles in the complex plane estimates of the various terms may be made. For the integration over $\Delta\mathbf{v}$, the solution is dominated by a pole corresponding to $2\Gamma+i\mathbf{k}_3\cdot\Delta\mathbf{v}$. This indicates that only small $\mathbf{k}_3\cdot\Delta\mathbf{v}$ are important. In addition, since $\mathbf{k}_1-\mathbf{k}_3\simeq 0$, the $\epsilon=+1$ term is a factor of $\kappa/\Delta\omega_D$ smaller than the $\epsilon=-1$ term (and hence for low fields can be ignored).

The effect of saturation, due to $\kappa\vartheta\neq 0$, leads to both a contribution from the $\epsilon=+1$ term and a power broadening effect. The most important pole, obtained from the denominator of A_{00} [see Eq. (B3)] corresponds to

$$i\mathbf{k}_1\cdot\mathbf{v}=\gamma=(\Gamma+\kappa\vartheta)[1-\kappa\vartheta^2/(\Gamma+\kappa\vartheta)(1+2\vartheta)]^{1/2}\ .$$

Thus the power broadening is comparable to $\kappa\vartheta$ and for this pole to be dominant we, of course, require that $\kappa\vartheta < \Delta\omega_D$.

Secondly, the motion washes out the spatial modulation, which corresponds to replacing $\cos^2[\mathbf{k}\cdot(\mathbf{x}-\mathbf{x}')]$ by $\frac{1}{2}$. This occurs since terms like

$$e^{\pm 2i\mathbf{k}_1\cdot\Delta\mathbf{v}t}$$

average to zero for times long compared to $1/\kappa$.

Thirdly, although we have approximately evaluated the $\Delta\mathbf{v}$ integral for large $\Delta\omega_D$ (compared to κ and Γ) we still have to perform the $\mathbf{v}$ integral. This leads to the replacement of Δ_2 by $(\Delta_2-\mathbf{k}_3\cdot\mathbf{v})$ and consequently, the reflectivity as a function of probe frequency is Doppler broadened. If the total width of order $\gamma_0=2\Gamma+\kappa+\kappa\vartheta+p$ is small compared to the Doppler width, near to line center the resulting Voigt profile is closely Gaussian and not strongly dependent on γ_0. The Lorentzian wings are only important where the profile has fallen to less than $\sim 1/\pi(\gamma_0/\Delta\omega_D)$ of its line center values and beyond about two Doppler widths. In this central region the terms associated with the products c_1T_3 and T_3c_2, as well as the $\kappa/2$ part of c_1, are smaller than c_1 or c_2 by the order of $(\Gamma+\kappa\vartheta)/\Delta\omega_D$. In addition, the terms corresponding to T_3 and T_4 are the order of $\kappa\vartheta/\Delta\omega_D$ and again small compared with unity.

The net result to lowest order in $(\Gamma+\kappa\vartheta)/\Delta\omega_D$ for the region close to line center (i.e., down to less than about $\gamma_0/\pi\Delta\omega_D$) gives the reflectivity proportional to $S(\Delta_2)$ where

$$S(\Delta_2)=\frac{\kappa\vartheta^2}{16\Delta\omega_D(1+2\vartheta)^3}\times\int d\mathbf{v}\frac{W(\mathbf{v})\gamma_0}{(\Delta_2-\mathbf{k}_3\cdot\mathbf{v})^2+\gamma_0^2}\times\left[\frac{1}{d^2(a+d)}\left\{a+\frac{a-d}{1+2a^2/\kappa(1+2\vartheta)}\right\}\right],\tag{22}$$

with $\gamma_0=2\Gamma+\kappa+\kappa\vartheta+p$,

$$a=[(\Gamma+\kappa\vartheta)]^{1/2}\ ,$$

$$d=\left[(\Gamma+\kappa\vartheta)-\frac{\kappa\vartheta^2}{(1+2\vartheta)}\right]^{1/2},$$

(i.e., $d<a$) and $\gamma=ad$.

For the approximation $\mathbf{k}_1\sim\mathbf{k}_3$ to be valid we require

$$|\mathbf{k}_1-\mathbf{k}_3|/|\mathbf{k}_1|\lesssim\frac{\kappa(1+\vartheta)}{\Gamma+\kappa\vartheta}\ .$$

For large p the above form may still be used. This form clearly demonstrates the Doppler broadening of the

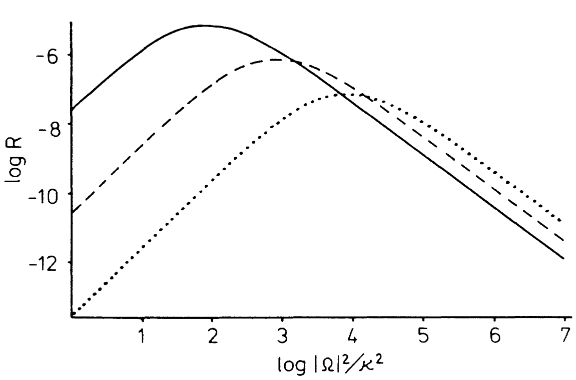

FIG. 4. Logarithmic plot of R against $|\Omega^2|/\kappa^2$ for $\Delta/\kappa=0$ and equal pump and probe bandwidths $b/\kappa=10^2$ (solid line), $b/\kappa=10^3$ (dashed line), and $b/\kappa=10^4$ (dotted line). The effect of finite probe bandwidth is seen by comparing this figure with Fig. 2(a) where $p=0$.

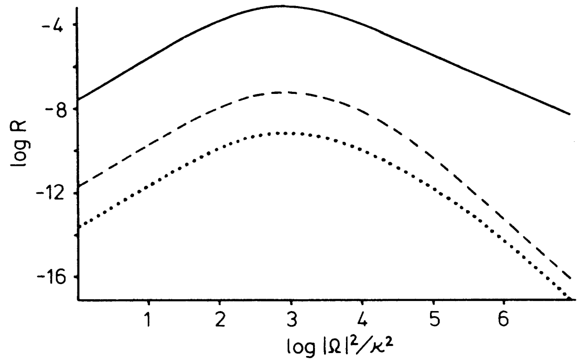

FIG. 5. Logarithmic plot of R against $|\Omega^2|/\kappa^2$ to show effects of atomic motion for $\Delta=0$, $p=0$, and $b/\kappa=10^3$. Doppler widths $\Delta_D/\kappa=0$, no atomic motion (solid line); $\Delta_D/\kappa=10^2$ (dashed line); and $\Delta_D/\kappa=10^3$ (dotted line).

probe response. Saturation now occurs as I^{-2} in contrast to the $I^{-3/2}$ dependence predicted by Eq. (21). This modified resonant response is shown in Fig. 5 for a laser bandwidth of $b/\kappa=10^3$ ($p=0$) and two values of Doppler width: $\Delta_D/\kappa=10^2$ and 10^3, together with the result obtained for no atomic motion. Note that Eq. (21) cannot be used in any form when Doppler motion occurs.

In conclusion, we have presented a theory of DFWM for cases where the pump laser bandwidth exceeds all other atomic relaxation rates. Our solution takes account of cross correlations in the atom-field products involved in the simultaneous averaging over space and the laser field fluctuations. The decorrelation approximation can only be used if all the averages are performed simultaneously. The effects of the laser bandwidth on the effective saturation intensity have been calculated for resonant and near resonant pump beams, showing a general trend for the effective saturation intensity to increase with increasing bandwidth. Our solution takes into account effects due to the spatial modulation induced in the nonlinear medium by the counterpropagating pump waves. In particular, if the resonantly excited atomic transitions $|g\rangle \rightarrow |e\rangle$ are saturated, these effects become important. We have shown also that the spectral width of the signal produced by broadband pumps and probed with a coherent or narrow-linewidth probe beam will be Doppler broadened in the presence of atomic motion. Our calculations apply to optically thin media. In the presence of strong absorption at the atomic line center the results will be significantly modified since the laser line shape will be dramatically altered as it propagates through the medium.

ACKNOWLEDGMENTS

Two of us, A.C. and D.R.M., are grateful to Science and Engineering Research Council (U.K.) for financial support. J.C. was supported in part by National Science Foundation Grants No. PHY86-04504 and No. INT86-02095 and the William Evans Fund while on leave at the University of Otago, New Zealand.

APPENDIX A

Combining Eqs. (12)–(14) we have

$$\langle \rho^{2,-1}(\mathbf{x},t)[\rho^{2,-1}(\mathbf{x}'t)]^* \rangle = \frac{|\Omega_3|^2}{16} e^{-\beta_3 t-\beta_3^* t} \int_{-\infty}^{t} dt_1 \int_{-\infty}^{t} dt_2 \int_{-\infty}^{t_1} dt_3 \int_{-\infty}^{t_3} dt_4 \int_{-\infty}^{t_2} dt_5 \int_{-\infty}^{t_5} dt_6$$
$$\times e^{\beta_3 t_1+\beta_3^* t_2} \Omega(\mathbf{x},t_1)\Omega^*(\mathbf{x}',t_2)[\Omega(\mathbf{x},t_3)e^{-\beta_2^*(t_3-t_4)}+\Omega(x,t_4)e^{-\beta(t_3-t_4)}]$$
$$\times[\Omega^*(x',t_5)e^{-\beta_2(t_5-t_6)}+\Omega^*(x',t_6)e^{-\beta^*(t_5-t_6)}]e^{-\alpha(t_1-t_3)-\alpha^*(t_2-t_5)} \ . \tag{A1}$$

In order to evaluate this integral we must decorrelate the rapidly fluctuating field terms. This can be done by writing

$$\langle \Omega(\mathbf{x},t_i)\Omega^*(\mathbf{x}',t_j)\Omega(\mathbf{x},t_k)\Omega^*(\mathbf{x}',t_l) \rangle = 2\Omega^4(e^{-b|t_i-t_j|-b|t_k-t_l|}+e^{-b|t_i-t_l|-b|t_j-t_k|}) \ , \tag{A2}$$

where we have made use of the phase-matching condition $\mathbf{k}_1+\mathbf{k}_2+\mathbf{k}_3+\mathbf{k}_4=\mathbf{0}$, and assumed a chaotic field with a Lorentzian line shape of half-width b, to give a sum of eight six-dimensional time integrals of the form

$$I_i=\Omega^4 \frac{|\Omega_3|^2}{8} e^{-2\Gamma t} \int_{-\infty}^{t} dt_1 \int_{-\infty}^{t} dt_2 \int_{-\infty}^{t_1} dt_4 \int_{-\infty}^{t_2} dt_5 \int_{-\infty}^{t_5} dt_6 e^{\beta_3 t_1+\beta_3^* t_2}$$
$$\times e^{-\beta_2^*(t_5-t_4)-\beta_2(t_5-t_6)-\alpha(t_1-t_3)-\alpha^*(t_2-t_5)-b|t_1-t_2|-b|t_3-t_5|} \ . \tag{A3}$$

Each of these integrals must be evaluated with due care over the ordering of the various times because of the $e^{-b|t_1-t_2|-b|t_3-t_5|}$ terms. This can be done analytically in the limit of large b, to order $1/b^2$, to give

$$\langle \rho^{2,-1}(\mathbf{x},t)[\rho^{2,-1}(\mathbf{x}',t)]^* \rangle = \frac{|\Omega_3|^2}{8}\Omega^4 \left\{ \frac{b^2}{b^2+\Delta^2}\frac{1}{b_2+\delta^2}\frac{1}{\Gamma^2\Delta_2^2}\frac{1}{\Gamma\kappa} + \frac{b^2}{b^2+\Delta^2}\frac{1}{b^2+\Delta^2}\frac{1}{\Gamma^2\kappa}\frac{\Gamma+\kappa}{(\Gamma+\kappa)^2+\Delta_2^2} + \frac{1}{\Gamma\kappa}\frac{b}{b^2+\Delta^2}\mathrm{Re}\left[\frac{1}{\Gamma+i\Delta_2}\frac{1}{\kappa+\Gamma+i\Delta_2}\left[\frac{1}{b-i\Delta}+\frac{1}{b-i\delta}\right]\right]\right\} . \tag{A4}$$

Because we have only included terms up to $1/b^2$ this expression is not valid for large values of detuning Δ. If $\Delta \sim b$ then all the terms presented here are of order $1/b^4$ and become comparable to those neglected in the integration. Therefore, in Eq. (15) given in the text we have simplified Eq. (A4) by setting $b \gg \Delta$.

APPENDIX B

In this Appendix we derive an expression for

$$\langle [\rho_{gg}^{0,0}-\rho_{ee}^{0,0}](\mathbf{x},t\to\infty)[\rho_{gg}^{0,0}-\rho_{ee}^{0,0}](\mathbf{x}',t\to\infty)\rangle$$

in order to demonstrate the eigenfunction expansion method[7] and decorrelation approximation we have used to derive Eq. (20).

We start from the nine density-matrix equations for the products

$$A_{00}(\mathbf{x},\mathbf{x}',t)=(\rho_{gg}^{0,0}-\rho_{ee}^{0,0})(\mathbf{x},t)(\rho_{gg}^{0,0}-\rho_{ee}^{0,0})(\mathbf{x}',t) ,$$

$$A_{10}(\mathbf{x},\mathbf{x}',t)=\rho_{eg}^{1,0}(\mathbf{x},t)(\rho_{gg}^{0,0}-\rho_{ee}^{0,0})(\mathbf{x}',t) ,$$

etc. If the weak probe beam is coherent and the counterpropagating pump waves are statistically independent and their fluctuations may be described within the PDM, we can easily derive from these nine equations the corresponding equations for the time evolution of the atom-field averages

$$A_{ij}^{(n_1,n_2)}(\mathbf{x},\mathbf{x}',t) .$$

In particular, we want to calculate $A_{00}^{(0,0)}(\mathbf{x},\mathbf{x}',t)$, whose equation of motion is given by

$$\left[\frac{d}{dt}+2\kappa\right]A_{00}^{(0,0)}(\mathbf{x},\mathbf{x}',t)=\kappa[\rho_0^{0,0}(\mathbf{x},t)+\rho_0^{0,0}(\mathbf{x}',t)]-2\,\mathrm{Im}[\Omega_1^*(\mathbf{x})A_{10}^{1,0}(\mathbf{x},\mathbf{x}',t)+\Omega_2^*(\mathbf{x})A_{10}^{0,1}(\mathbf{x},\mathbf{x}',t) -\Omega_1(\mathbf{x}')A_{02}^{-1,0}(\mathbf{x},\mathbf{x}',t)-\Omega_2(\mathbf{x}')A_{02}^{0,-1}(\mathbf{x},\mathbf{x}',t)] ,$$

with

$$\Omega_1(\mathbf{x})=\Omega e^{i\mathbf{k}_1\cdot\mathbf{x}},\quad \Omega_2(\mathbf{x})=\Omega e^{-i\mathbf{k}_1\cdot\mathbf{x}} . \tag{B1}$$

In the equations for $A_{10}^{(1,0)}(\mathbf{x},\mathbf{x}',t)$, etc., we keep only couplings to atom-field averages with $n_1=n_2=0$. All other couplings can certainly be neglected in the broad-bandwidth limit. This procedure corresponds to a decorrelation approximation and yields, e.g.,

$$\left[\frac{d}{dt}-i\Delta+\Gamma+\kappa+b\right]A_{10}^{(1,0)}=\frac{i}{2}\Omega_1(\mathbf{x})A_{00}^{(0,0)}(\mathbf{x},\mathbf{x}',t) -i\Omega_1(\mathbf{x}')A_{12}^{(0,0)}(\mathbf{x},\mathbf{x}',t) +\kappa\rho_1^{1,0}(\mathbf{x},t) . \tag{B2}$$

As indicated in the text, similar equations are obtained by using the method of Georges[6] for either phase-diffusing or chaotic fields. Physically, this decorrelation approximation takes into account only the dependence of atom-field averages of the type $\langle \Omega(\mathbf{x})A_{10}\rangle$ which determine $\langle A_{00}\rangle$. The equations for $\langle \Omega(\mathbf{x})A_{10}\rangle$ are then decorrelated to give products such as $\langle \Omega(\mathbf{x})\Omega^*(\mathbf{x}')\rangle\langle A_{00}\rangle$, etc., [and assuming $\langle \Omega(\mathbf{x})\Omega(\mathbf{x}')\rangle = \langle \Omega^*(\mathbf{x})\Omega^*(\mathbf{x}')\rangle = 0$].

Proceeding with the equation for $A_{12}^{(0,0)}(\mathbf{x},\mathbf{x}',t)$ and the various density-matrix elements

$$\rho_1^{n_1,n_2}(\mathbf{x},t) ,$$

in a similar way, we finally obtain in the broad-bandwidth limit

$$\langle A_{00}(\mathbf{x},\mathbf{x}',t\to\infty)\rangle = \frac{\langle(\rho_{gg}^{0,0}-\rho_{ee}^{0,0})(\mathbf{x},t\to\infty)\rangle^2}{1-\dfrac{2\kappa}{\Gamma}\dfrac{\vartheta^2\cos^2[\mathbf{k}_1\cdot(\mathbf{x}-\mathbf{x}')]}{(1+2\vartheta)\left[1+\dfrac{\kappa}{\Gamma}\vartheta\right]}} , \tag{B3}$$

with the stationary mean population inversion

$$\langle(\rho_{gg}^{0,0}-\rho_{ee}^{0,0})(\mathbf{x},t\to\infty)\rangle = \frac{1}{1+2\vartheta} . \tag{B4}$$

From Eq. (B2) we notice that the large-bandwidth result is independent of the higher-order statistics of the laser fluctuations. Owing to correlations

$$\langle A_{00}(\mathbf{x},\mathbf{x}',t\to\infty)\rangle \neq \langle(\rho_{gg}^{0,0}-\rho_{ee}^{0,0})(\mathbf{x},t\to\infty)\rangle^2 .$$

*Present address: Schuster Laboratory, University of Manchester, Manchester, United Kingdom.

[1]G. Alber, J. Cooper, and P. Ewart, Phys. Rev. A **31**, 2344 (1985).
[2]*Optical Phase Conjugation,* edited by R. A. Fisher (Academic, New York, 1983).
[3]J. E. Reinjes, *Nonlinear Optical Parametric Processes in Liquids and Gases* (Academic, New York, 1984).
[4]L. A. Rahn, R. L. Farrow, and R. P. Lucht, Opt. Lett. **9**, 223 (1984); R. J. Hall and D. A. Greenhalgh, J. Opt. Soc. Am. B **3**, 1637 (1986); P. Narum, M. D. Skeldon, and R. W. Boyd, IEEE J. Quantum Electron. **QE-22**, 2161 (1986).
[5]R. L. Abrams and R. C. Lind, Opt. Lett. **2**, xxx (19xx).
[6]T. Georges, Phys. Rev. A **21**, 2034 (1980).
[7]P. Zoller, Phys. Rev. A **20**, 1019 (1979).